Available online at www.sciencedirect.com
SCIENCE DIRECT
Nuclear Instruments and Methods in Physics Research A 558 (2006) 25–31
NUCLEAR INSTRUMENTS & METHODS IN PHYSICS RESEARCH Section A
www.elsevier.com/locate/nima

Computational needs for the RIA accelerator systems ☆

P.N. Ostroumov*, J.A. Nolen, B. Mustapha

Physics Division, Argonne National Laboratory, 9700 S. Cass Ave., Argonne, IL 60439, USA

Available online 28 November 2005

Abstract

This paper discusses the computational needs for the full design and simulation of the RIA accelerator systems. Beam dynamics simulations are essential to first define and optimize the architectural design for both the driver linac and the post-accelerator. They are also important to study different design options and various off-normal modes in order to decide on the most-performing and cost-effective design. Due to the high-intensity primary beams, the beam-stripper interaction is a source of both radioactivation and beam contamination and should be carefully investigated and simulated for proper beam collimation and shielding. The targets and fragment separators area needs also very special attention in order to reduce any radiological hazards by careful shielding design. For all these simulations parallel computing is an absolute necessity.

PACS: 29.17.+w; 29.27.−a; 41.75.−i

Keywords: RIA simulations; Beam dynamics; Stripper modeling; Target simulations; Fragment separators

1. Introduction

The Rare Isotope Accelerator (RIA) is a next generation facility for basic research with intense beams of radioactive and rare isotopes [1]. To produce such beams RIA will use primary beams of any ion from protons (up to 1 GeV) to uranium (up to $400\,\mathrm{MeV}/u$) with beam power up to 400 kW. RIA is based on two CW superconducting (SC) linacs, a 1.4-GV driver designed to simultaneously accelerate multiple-charge-state heavy-ion beams and a ~140-MV post-accelerator designed for the efficient acceleration starting from singly charged secondary beams with masses up to $A = 240$ from ion source energies. To meet the facility requirements RIA will also include state-of-the-art electron cyclotron resonance (ECR) ion sources for the production of high-intensity heavy-ion beams, two stripping stations for beams of heaviest ions, high-power ISOL and fragmentation targets, high-resolution fragment and isobar separators and transport systems for beams with large momentum and charge spread. RIA will also have a new production scheme combining both the fragmentation and the ISOL methods by thermalizing fast radioactive ions in a gas catcher [2] to produce low-energy good-quality secondary beams. Fig. 1 shows a schematic layout of the RIA facility including four experimental areas with different secondary beam energies serving different experimental programs from Ion Traps to Astrophysics to Nuclear Structure to high-energy Nuclear Reactions.

RIA has recently been ranked as the third highest priority for future Scientific Facilities in the 20 year plan of the US Department of Energy (DOE) [3]. Following this high ranking, the RIA project received a preliminary approval (CD-0: critical decision 0) from the DOE. The research and development (R&D) for RIA involves many national laboratories and universities. An impressive progress has been made over the last few years in the different areas of RIA R&D from the ion source [4] to the driver linac [5] to the different targets [6] and fragment separators [7] to the post-accelerator [8]. In this paper, we discuss the computational needs for the full design and simulation of the RIA accelerator systems. In the next section, we review both the existing and newly developed

☆This work is supported by the U.S. Department of Energy under contract W-31-109-Eng-38.
*Corresponding author. Tel.: +1 630 252 4897; fax: +1 630 252 9647.
E-mail address: ostroumov@phy.anl.gov (P.N. Ostroumov).

0168-9002/$ - see front matter © 2005 Elsevier B.V. All rights reserved.
doi:10.1016/j.nima.2005.11.034

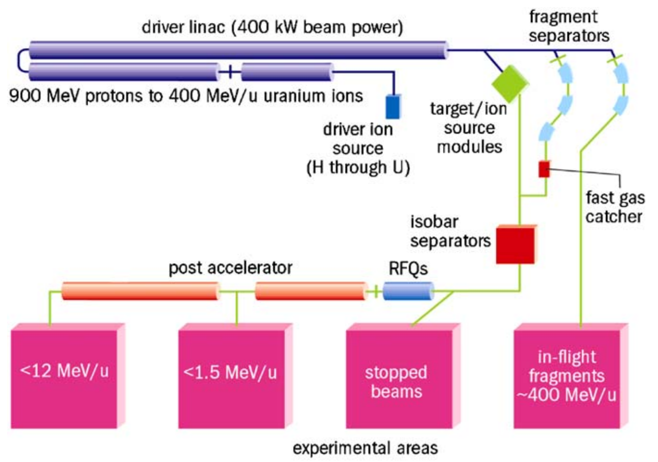

Fig. 1. Schematic layout of the RIA facility showing the three sections of the driver linac starting from the ion source, the three radioactive isotope production schemes and the four experimental areas.

tools for both accelerator design and beam dynamic simulations emphasizing the need to fully describe the new features of the RIA driver linac. In Section 3, we consider the beam-stripper interaction including elastic and inelastic interactions and the subsequent need for beam collimation and shielding. In Section 4, we discuss the production and separation of radioactive isotopes emphasizing the aspect of radioactive ion release from ISOL targets and the radiological and shielding aspects for both the ISOL and fragmentation targets.

2. Beam dynamics

2.1. Goal and scope

The ultimate goal of the beam dynamics simulations is to define the overall architectural designs for both the driver linac and the post-accelerator that satisfy the facility requirements. End-to-end simulations are necessary to study the performance and limitations of different design options in order to decide on the most-performing and cost-effective design. In order to fulfill these goals the end-to-end simulations should include:

- Up-to-date heavy-ion beam physics.
- Multiple charge state acceleration necessary to reach the high intensity goal.
- Stripper effects on the dynamics of heaviest ion beams.
- Automatic corrective steering required for simulations with errors.
- Capability of determining both the fractions and locations of any beam loss in order to optimize the design and define the tolerance to different errors.
- Capability of studying possible failure modes and ways to restore the beam by automatic retuning of the accelerator excluding the failing elements.

2.2. Tools for element and section design and optimization

For accelerator element design including RF cavities and the calculation of the corresponding 3D electromagnetic fields, codes such as Microwave Studio, Electromagnetic Studio and MAFIA from CST [9], ANSYS [10], Poisson/Superfish [11] and HFSS (High-Frequency Structure Simulator) [12] may be used. Recently, we have used the advanced electromagnetic code Omega-3P developed by the SLAC group [13] for more precise resonator design.

For the design of the different sections of the SC Linac including optimization and beam matching, matrix-based codes such as TRANSPORT [14], TRACE3D [15], COSY [16] and GIOS [17] are often used. For the RT front-end structure, codes like DYNAMION [18] and PARMTEQ [19] may be used.

2.3. Codes for full design and end-to-end simulations

A few years ago, none of the existing beam dynamics codes was able to fully describe the beam dynamics in all the elements of the RIA accelerator systems and more importantly the new features of the driver linac like multiple-charge-state acceleration and stripper simulation. A great effort has been made during the last few years toward developing new codes that allow detailed studies and end-to-end simulations of the RIA driver linac. Two new ray-tracing codes have been specially developed: the LANA code originally developed at the Institute for Nuclear Physics INR-Moscow [20] and currently supported at Michigan State University and the TRACK code [21] developed at Argonne National Laboratory. Both codes have been used to perform detailed simulations of the SC linac sections and produced similar overall results except in some of the details. For an independent validation of the two codes, an effort is currently under way to modify the existing codes PARMTEQ and IMPACT [22] for the simulation of heavy-ion beams in RIA-type accelerators. Initial comparisons of energy gain and beam second moments in the high-energy section of the RIA driver linac show very good agreement [23] with the code TRACK.

2.4. Simulations of two linac options using TRACK

Since the first simulations [24] the code TRACK has undergone many updates and further development [25] to either include new features or refine some of the existing ones. Among these updates we cite:

- Realistic space charge effects of multi-component ion beams.
- Realistic stripper effects including thickness fluctuations on the beam properties.
- End-to-end simulation of the driver linac starting from the ion source.
- Randomly generated misalignment and RF errors.

- Automatic and realistic beam steering based on beam position monitors.
- Capability of determining the fractions and locations of eventual beam losses.
- Parallel computing on multi-processor machines.

Fig. 2 shows the evolution of the beam envelopes along the driver linac starting from the ECR ion source to the target (bottom) as well as the particle coordinates of the 5 charge state uranium beam at the target location (top). Using this powerful simulation tool we have performed extensive simulations of two linac design options including different sources of errors on the parallel computer cluster Jazz [26] at Argonne. The goal of these simulations was first to identify the most critical errors, second to establish an error budget based on beam loss analysis and finally to compare the performances and limitations of the two linac options. The first linac option is the original Baseline design described in [5] and the second is the Triple-spoke design where the elliptical-cell cavities in the high-energy section of the linac are replaced by the triple-spoke cavities under development now at ANL [27].

Table 1 lists the errors used in these simulations and their typical amplitudes. Simulating 50 random sets (10 million particles) for each individual error and comparing to the case with no errors, we were able to identify the RF field and phase errors and the fluctuations in the strippers thicknesses as the most critical errors. For further investigation and beam loss analysis of both designs we simulated different combinations of these errors keeping other errors at their values of Table 1. Table 2 lists the different combinations of RF errors and stripper thickness fluctuations. For each combination, 200 random sets of errors were simulated with 2×10^5 particles each (a total of 40 million particles). Increasing the error amplitudes from combination 1 to 6, we noticed an increase in the longitudinal emittances for both the Baseline and the Triple-spoke designs. The Baseline design showed more sensitivity with an increase in the transverse beam emittances not observed for the Triple-spoke design. This increase in the transverse emittances reflects a possible coupling between the transverse and longitudinal motion which resulted into an increasing beam loss in the Baseline design [25]. Whereas no beam losses were observed for the Triple-spoke design even in the case of the highest errors (combination 6). Fig. 3 shows beam losses in W/m along the driver linac for both the Baseline and the Triple-spoke designs. The first two peaks on each plot correspond to the losses at the two strippers which are controlled losses to be stopped at the collimators following the strippers. For the Baseline design, uncontrolled losses are observed in the high-energy section. They are negligible for combinations 1&2, approaching the 1 W/m limit for hands-on maintenance for combinations 3&4 and about 10 W/m for combinations 5&6. Whereas no uncontrolled losses were observed for the Triple-spoke design. From these studies we conclude that the Baseline design has more limitations concerning beam losses and that the Triple-spoke design is more tolerant of errors.

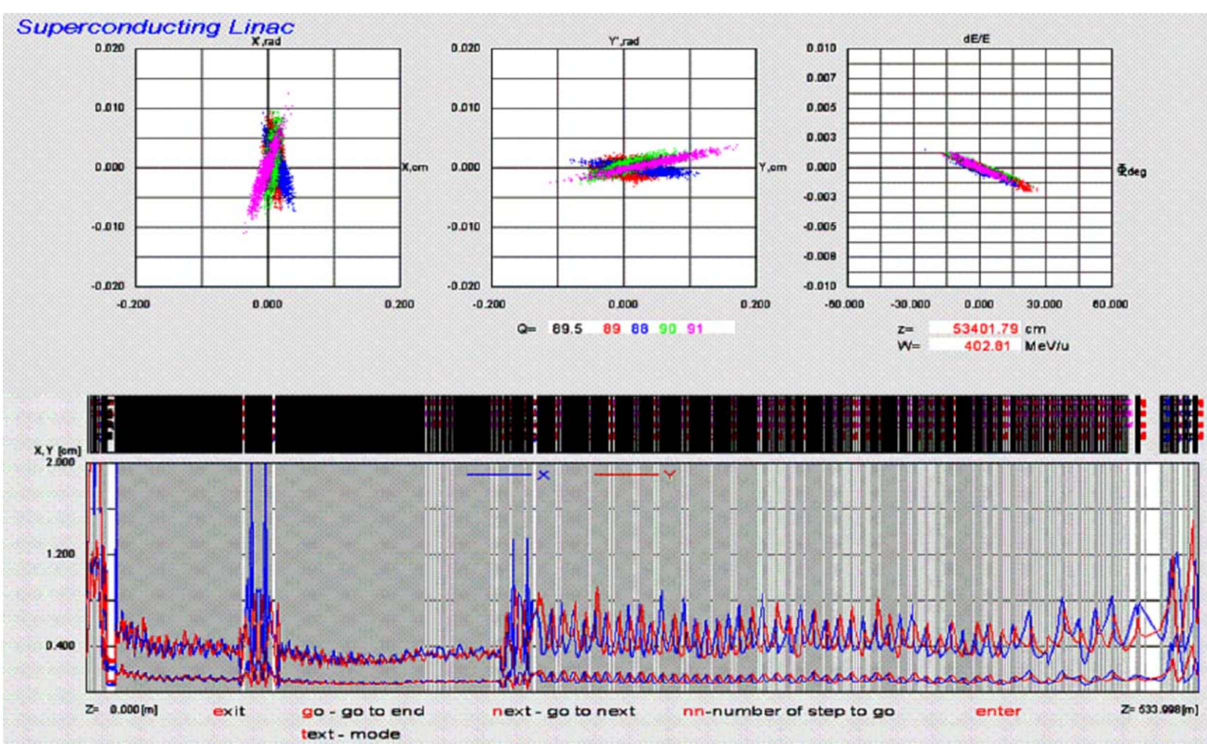

Fig. 2. End-to-end simulation of the baseline driver linac showing beam envelopes throughout the linac (bottom) and the phase–space plots of the multi-charge states beam at the linac exit (top).

Table 1
Different sources of error and their typical values

Error	Description	Value	Distribution
1	Cavity end displacements	0.05 cm (max.)	Uniform
2	Solenoid end displacements	0.015–0.05 cm (max.)	Uniform
3	Quadrupole end displacements	0.01 cm (max.)	Uniform
4	Quadrupole rotation	2 mrad (max.)	Uniform
5	Cavity field error	0.5% (r.m.s.)	Gaussian
6	Cavity phase error	0.5° (r.m.s.)	Gaussian
7	Stripper thickness fluctuation	5–10% (FWHM)	Gaussian

Table 2
Combinations of RF errors and stripper thickness fluctuations used to study beam dynamics and beam losses

Combination	RF errors	Thickness fluctuation
1	Field: 0.3%, Phase: 0.3°	5% FWHM
2	Field: 0.3%, Phase: 0.3°	10% FWHM
3	Field: 0.5%, Phase: 0.5°	5% FWHM
4	Field: 0.5%, Phase: 0.5°	10% FWHM
5	Field: 0.7%, Phase: 0.7°	5% FWHM
6	Field: 0.7%, Phase: 0.7°	10% FWHM

2.5. *Future code development*

The goal of future code development is to develop a complete accelerator set-up tool based on an accurate and realistic computer model. Experience at many operating machines showed that such models are essential and save both machine time and manpower. The main future development is to develop a longitudinal phase setting procedure for multi-charge state beams in order to:

- Account for cavity-dependent field levels which is inherent to a linac comprising a large number of SC resonators.
- Minimize the effective beam emittance at the stripper location.
- Produce tunes for ions with different q/A ratios to maximize the output energy.
- Develop off-normal tunes to compensate for missing resonators after an eventual failure.

Along with the longitudinal tuning procedure, a procedure for the optimization of the beam transverse envelopes is also necessary in order to:

- Determine optimum focusing fields to minimize the beam envelopes.
- Produce transverse tunes for ions with different q/A ratios.
- Retune the accelerator after a failure excluding the failing resonators and or focusing elements.

3. Strippers

Stripping is necessary to reach intermediate and high energies in heavy-ion accelerators. By increasing the ions q/A ratio, the acceleration to higher energies is more efficient and more importantly more cost-effective. However, stripping will affect both the beam intensity and quality. In the beam-stripper interactions we distinguish between elastic and inelastic processes. Elastic interactions include atomic and elastic nuclear interactions which could change the charge, the energy and the angle of the incident ion but not the ion specie. Inelastic interactions are nuclear reactions which could produce radioactive products.

Charge exchange or electron stripping is the process responsible of producing the charge state distribution of the beam after a stripper. Semi-empirical formulas and Monte-Carlo codes are available to estimate the required stripper thickness and calculate the charge state distribution. From these we cite the set of formulas originally developed by Baron et al. [28] and later updated by Leon et al. [29], the code ETACHA [30] and the code GLOBAL [31] which is more valid for energies above 100 MeV/u. In the case of RIA, a comparative study [32] of these formulas and codes for uranium beams led to the necessity of experimental measurements at the exact stripping energies. These measurements have already been performed with 11 MeV/u uranium at Texas A&M University, 85 MeV/u uranium at GSI-Darmstat and 80 MeV/u bismuth at Michigan State University. Analysis of the data is under way.

Multiple Coulomb scattering with both the electrons and atoms of the stripping medium is the process responsible for the energy (energy loss and straggling) and angle (angular straggling) distributions of the beam after a stripper. For particle tracking codes like TRACK, it is important to have the correlated energy and angle distributions including the respective tails. A Monte-Carlo code such SRIM [33] may be used, however, when compared with data the calculated energy-loss straggling is 5–7 times smaller. We believe that this is due to the fact that SRIM does not include any fluctuations in the stripper thickness or the ion charge state which could be responsible for the extra-broadening of the energy peak. In order to include these effects and for fast generation of the correlated energy and angle distributions ion by ion we opt for the parameterization of SRIM results for a uranium beam and both strippers [25]. An event generator based on these parameterization is now used by the code TRACK. We are currently developing a more general stripper model for any beam-stripper combination.

The simultaneous acceleration of multiple charge states in the RIA driver linac will not only reduce the losses at the strippers but also reduce the need for shielding. However, due to the high intensity, radioactivation and possible

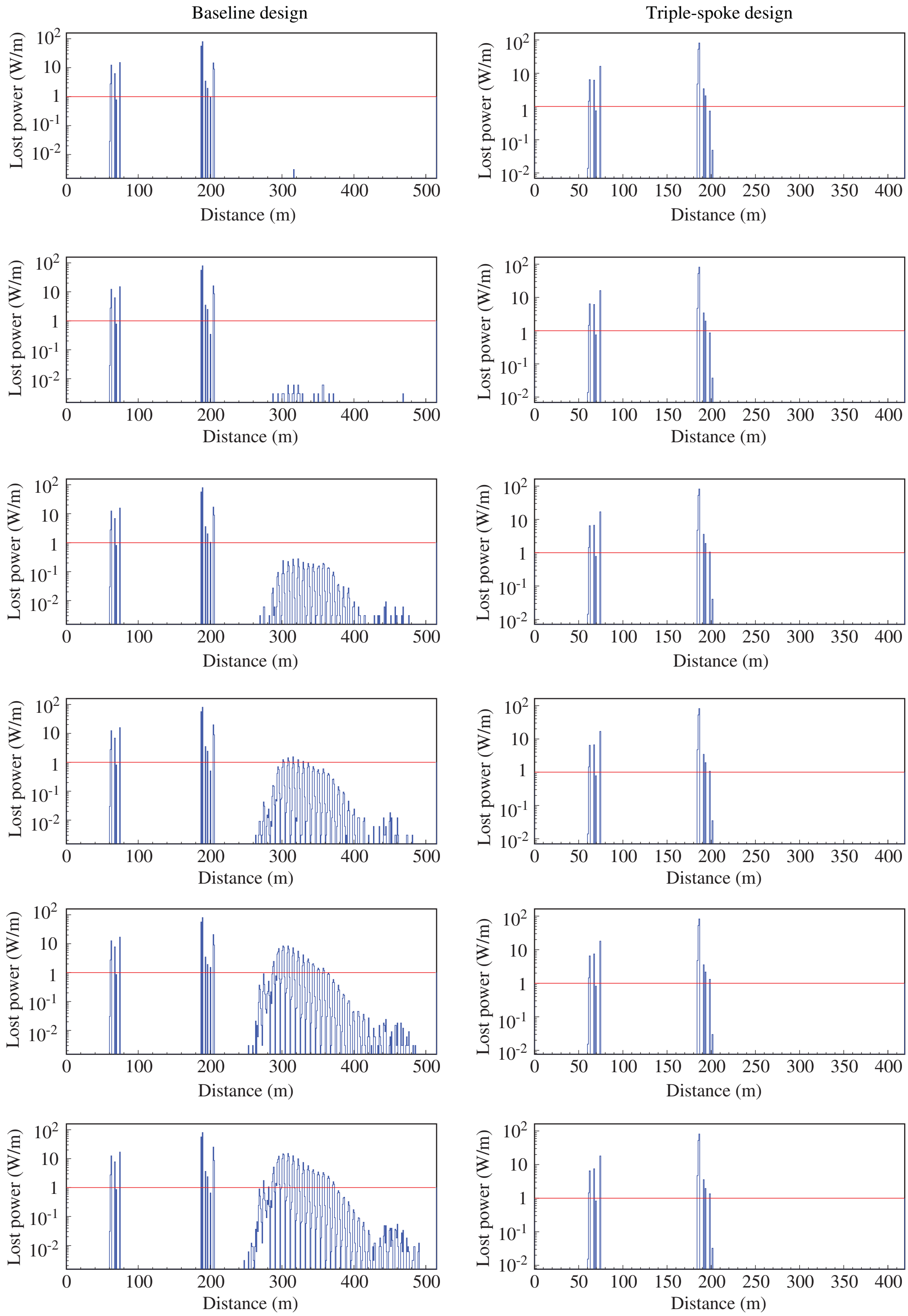

Fig. 3. Beam power lost along the accelerator in W/m for both the baseline and Triple-spoke design and the error combinations of Table 2. The plots are for combination 1 (top) to combination 6 (bottom), respectively. The horizontal line shows the 1 W/m limit to not exceed for hands-on maintenance. The first two peaks on each figure correspond to the losses at the two strippers which are controlled losses.

beam contamination by nuclear reactions products become an issue. Knowing the fractions and distributions of these radioactive products is very important for the appropriate design of beam collimation and shielding. Depending on the stripper material and the beam energy and mass, different mechanisms of inelastic interactions may take place. They become more important at energies $>50\,\mathrm{MeV}/u$. The dominant processes are the fragmentation for most heavy ions and fission for the heaviest ones. In order to determine the interacting beam fraction and the nuclei produced by fragmentation, we may use the semi-empirical formula EPAX [34] for production yields. EPAX is energy-independent and most valid at higher energies. Monte-Carlo codes based on the two-step model consisting of an Intra-Nuclear Cascade step (ISABEL [35], INCL [36],...) followed by a Fission-Evaporation step (ABLA [37], PACE [38],...) are available and may be used. A Recently developed heavy-ion-reactions event generator LAQGSM [39] seems to be promising. In addition to the production yields these codes could also produce full energy and momentum distributions of the fragments. This information could be used for further tracking using a beam dynamics code in order to study related beam losses and possible beam contamination. We are currently investigating these issues. For the design of beam dumps and shielding, codes such MCNPX [40] and MARS [41] may be used. For both codes, development is under way to include heavy-ion capabilities, by incorporating the LAQGSM event generator. A newly developed particle and heavy-ion transport code PHITS [42] is also used. Monte-Carlo tracking of heavy-ion reactions products with such general purpose codes will be very computer-intensive and require parallel processing.

4. Targets and fragment separators

Targets have a lot in common with strippers except that they will receive a much higher beam power due to the higher energy and more importantly that most of the beam will be stopped. Only a fraction of the secondary beam (the selected isotope) is to be transmitted for immediate use or re-acceleration.

In the case of ISOL targets where a light-ion beam is incident on a thick target of a heavy element, the beam will be stopped in the target. To handle such high beam powers (up to 400 kW) two target design options are been developed: the two-step target [43] and the tilted-foil target [44]. In both cases, the reaction products have to first diffuse through the target material then effuse through the target enclosure to be ionized in an ion source and extracted. This process known as the release process is chemical dependent and require the use of an isobar separator to select a given isotope. We have recently developed a Monte-Carlo code package to simulate the release process [45] where the diffusion is based on a theoretical model [46]. The effusion is simulated by tracking the produced ions inside the target-ion source system [47] using the geometry and tracking capabilities of Geant-4 [48]. These targets will be very hot and radioactive, appropriate cooling and shielding are absolutely required. Prototyping as well as code development for full simulations of these two aspects are under-way.

In the case of fragmentation targets where a heavy-ion beam is incident on a thin target of a light element, up to a third of the beam power will be deposited in the target. A windowless flowing liquid-lithium target has already been built and tested for this purpose [49]. In this case, the non-interacting primary beam and the secondary beam (of all reaction products) will leave the target into a small angle cone with energies close to the primary beam energy. A fragment separator will be used to first deflect the non-interacting beam into a beam dump and second to separate and select the isotope of interest from the rest of the beam which should also be stopped in specially designed beam stops. Although the demonstration of the liquid-lithium target solved the problem of power dissipation in the target, the problems of power dissipation and induced radioactivity in the fragment separator and its beam dumps are yet to be investigated. For beam dumps and shielding, the same codes as for the stripper areas (MNCPX and MARS after developing heavy-ion capabilities as well as the code PHITS) could be used.

5. Summary

The basic design and simulation tools for the RIA accelerator systems exist. Parallel computing is vital for extensive simulations of the full system. Further code development is under way in all areas: accelerators, strippers, targets and fragment separators.

References

[1] J.A. Nolen, Nucl. Phys. A 734 (2004) 661.
[2] G. Savard, et al., Nucl. Instr. and Meth. B 204 (2003) 582.
[3] DOE Office of Science web site @ ⟨http://www.sc.doe.gov⟩.
[4] D. Leitner, ECR Ion sources for RIA, RIA Facility Workshop, March 9–13, 2004, Organized jointly by the NSCL and the ANL Physics Division @ ⟨http://meetings.nscl.msu.edu/ria2004/talks_dl.php⟩.
[5] P.N. Ostroumov, Phys. Rev. ST. Accel. Beams 5 (2002) 030101.
[6] J.A. Nolen, et al., Nucl. Phys. A 701 (2002) 312c.
[7] B.M. Sherrill, Fragment Separator at RIA, RIA Facility Workshop, March 9–13, 2004, Organized jointly by the NSCL and the ANL Physics Division @ ⟨http://meetings.nscl.msu.edu/ria2004/talks_sbd.htm⟩.
[8] P.N. Ostroumov, et al., in: Proceedings of the RIA R&D Workshop, Washington, DC, August 26–28, 2003 @ ⟨http://www.c-ad.bnl.gov/RIA⟩, paper 2.4.3.
[9] CST, Darmstadt, Germany web site @ ⟨http://www.cst.de/⟩.
[10] ANSYS web page @ ⟨http://www.ansys.com⟩.
[11] Poisson/Superfish, LAACG' web page @ ⟨http://laacg1.lanl.gov⟩.
[12] HFSS, ANSOFT web page @ ⟨http://www.ansoft.com⟩.
[13] Y. Sun, Ph.D. Thesis, Stanford University, 2002.
[14] K.L. Brown, The ion optical program TRANSPORT, Technical Report 91, SLAC, 1979.
[15] K.R. Crandall, TRACE 3-D documentation, Report LA-11054-MS, Los Alamos, 1987.
[16] M. Berz, COSY INFINITY, Version 8 User's Guide and Reference Manual, MSU, 1999.
[17] H. Wollnik, J. Brezina, M. Berz, Nucl. Instr. and Meth. A 258 (1987) 408.
[18] A.A. Kolomiets, et al., in: S. Myers, et al. (Eds.), Proceedings of the Sixth European Particle Accelerator Conference, Stockholm, Sweden, June 22–26, 1998, p. 1201.

[19] T.P. Wangler, et al., in: Proceedings of the RIA R&D Workshop, Washington, D.C., August 26–28, 2003 @ ⟨http://www.c-ad.bnl.gov/RIA⟩, paper 2.0.1.
[20] D.V. Gorelov, P.N. Ostroumov, in: R. Pascual (Ed.), Proceedings of the Fifth European Particle Accelerator Conference, Universitat Autonoma de Barcelona, Sitges, Spain, 1996, p. 1271.
[21] P.N. Ostroumov, V.N. Aseev, TRACK—a code for beam dynamics simulation in SC linac with 3D electric and magnetic fields, ANL Technical report, 2003.
[22] R.D. Ryne, et al., MaryLie/IMPACT: A Parallel Beam Optics Code with Space Charge, ICAP 2002 Abstracts and Posters @ ⟨http://icap02.pa.msu.edu/papers/⟩.
[23] R.D. Ryne, et al., in: Proceedings of the RIA R&D Workshop, Washington, D.C., August 26–28, 2003 @ ⟨http://www.c-ad.bnl.gov/RIA⟩, paper 2.0.2.
[24] P.N. Ostroumov, Phys. Rev. ST. Accel. Beams 3 (2000) 030101.
[25] P.N. Ostroumov, V.N. Aseev, B. Mustapha, Phys. Rev. ST. Accel. Beams 7 (2004) 090101.
[26] Jazz, LCRC web page @ ⟨http://www.lcrc.anl.gov⟩.
[27] K.W. Shepard, et al., Phys. Rev. ST Accel. Beams 6 (2003) 080101.
[28] E. Baron, et al., Nucl. Instr. and Meth. A 328 (1993) 177.
[29] A. Leon, et al., At. Data Nucl. Data Tables 69 (1998) 217.
[30] J.P. Rozet, et al., Nucl. Instr. and Meth. B 107 (1996) 67.
[31] C. Scheidenberger, et al., Nucl. Instr. and Meth. B 142 (1998) 441.
[32] M. Portillo, Ph.D. Thesis, Michigan State University, 2002.
[33] J.F. Ziegler, J.P. Biersack, U. Littmark, The Stopping and Range of Ions and Solids, Pergamon Press, NY, 1996. The code SRIM @ ⟨www.srim.org⟩.
[34] K. Summerer, B. Blank, Phys. Rev. C 61 (2000) 034607.
[35] Y. Yariv, Z. Fraenkel, Phys. Rev. C 20 (1979) 2227.
[36] J. Cugnon, Nucl. Phys. A 462 (1987) 751.
[37] J.J. Gaimard, K.-H. Schmidt, Nucl. Phys. A 531 (1991) 709.
[38] A. Gavron, Phys. Rev. C 21 (1980) 230.
[39] K.K. Gudima, S.G. Mashnik, A.J. Sierk, User Manual for the code LAQGSM, LANL Report LA-UR-01-6804 @ ⟨http://lib-www.lanl.gov/la-pubs/00818645.pdf⟩.
[40] L. Waters, MCNPX web page @ ⟨http://www.mcnpx.lanl.gov⟩
[41] N.V. Mokhov, MARS web page @ ⟨http://www-ap.fnal.gov/MARS⟩
[42] H. Iwase, et al., J. Nucl. Sci. Tech. 39 (2002) 1142.
[43] M. Portillo, et al., Nucl. Instr. and Meth. B 194 (2002) 193.
[44] B. Mustapha, J.A. Nolen, I.C. Gomes, Nucl. Phys. A 746 (2004) 437c.
[45] B. Mustapha, J.A. Nolen, Nucl. Instr. and Meth. B 204 (2003) 286.
[46] J. Crank, The Mathematics of Diffusion, Clarendon Press, Oxford, 1975.
[47] B. Mustapha, J.A. Nolen, Nucl. Instr. and Meth. A 521 (2004) 59.
[48] Geant-4 web page @ ⟨http://geant4.web.cern.ch/geant4/⟩.
[49] C.B. Reed, J.A. Nolen, J.R. Specht, V.J. Novick, P. Plotkin, Nucl. Phys. A 746 (2004) 161c.